

Metal-coated hollow nanowires for low-loss transportation of plasmonic modes with nanoscale mode confinement

This content has been downloaded from IOPscience. Please scroll down to see the full text.

2012 J. Opt. 14 095501

(<http://iopscience.iop.org/2040-8986/14/9/095501>)

View [the table of contents for this issue](#), or go to the [journal homepage](#) for more

Download details:

IP Address: 130.199.3.165

This content was downloaded on 11/06/2014 at 23:12

Please note that [terms and conditions apply](#).

Metal-coated hollow nanowires for low-loss transportation of plasmonic modes with nanoscale mode confinement

Yalin Su^{1,2}, Zheng Zheng¹, Yusheng Bian¹, Lei Liu¹, Xin Zhao¹, Jiansheng Liu¹, Tao Zhou³, Shize Guo², Wei Niu², Yulong Liu² and Jinsong Zhu⁴

¹ School of Electronic and Information Engineering, Beihang University, Beijing 100191, People's Republic of China

² Northern Institute of Electronic Equipment, Beijing 100083, People's Republic of China

³ Department of Physics, New Jersey Institute of Technology, Newark, NJ 07102, USA

⁴ National Center for Nanoscience and Technology, No. 11 Zhongguancun Beiyitiao, Beijing 100190, People's Republic of China

E-mail: zhengzheng@buaa.edu.cn

Received 5 April 2012, accepted for publication 3 August 2012

Published 24 August 2012

Online at stacks.iop.org/JOpt/14/095501

Abstract

Two types of plasmonic waveguiding structures based on hollow dielectric nanowires are proposed and their modal properties are investigated numerically at a wavelength of 1550 nm. The first type of waveguide consists of a high-index hollow nanowire covered directly by a thin metallic film. Depending on the size of the hollow nanowire, such a waveguide could support a plasmonic mode with lower propagation loss than the metal-coated nanowire structures without a hollow core. To further reduce the propagation loss, a second type of waveguide is proposed, which includes an additional low-index silica buffer layer between the metal layer and the hollow nanowire. Simulations reveal that the additional low-index buffer could enable strong hybridization between the dielectric mode and the plasmonic mode, which leads to even lower propagation loss while maintaining nanoscale confinement similar to that of the first type of waveguide. Both of the proposed waveguides are feasible using modern fabrication methods and could facilitate potential applications in integrated photonic components and circuits.

Keywords: waveguide, surface plasmon, hollow nanowire, integrated photonics

(Some figures may appear in colour only in the online journal)

1. Introduction

Plasmonic waveguiding structures are playing an increasingly important role in a wide range of areas [1]. Guiding and confining lightwaves at the sub-wavelength scale beyond the fundamental diffraction limit have been enabled by the surface plasmon polaritons (SPPs), laying the groundwork for the realization of highly integrated photonic components and circuits with complex functions [2]. Numerous kinds of plasmonic waveguides have been proposed and demonstrated, including metal nanowires [3], long-range SPP waveguides [4, 5], metal slot structures [6–9], metallic V grooves [10] and

wedges [11], cylindrical metal nanowire waveguides [12, 13], dielectric-loaded plasmonic waveguides [14, 15] as well as the recently studied hybrid plasmonic structures [16–28].

On the other hand, silicon based plasmonic waveguides have attracted particular interest [29], due to their high compatibility with the standard CMOS technology and potential for further on-chip integrations [30]. However, structures with metal directly deposited on the silicon waveguide may have very high optical loss. One commonly employed method for loss reduction is to separate the metal layer and the silicon structure by introducing an additional low-index buffer layer [18, 19, 31–36] or incorporating

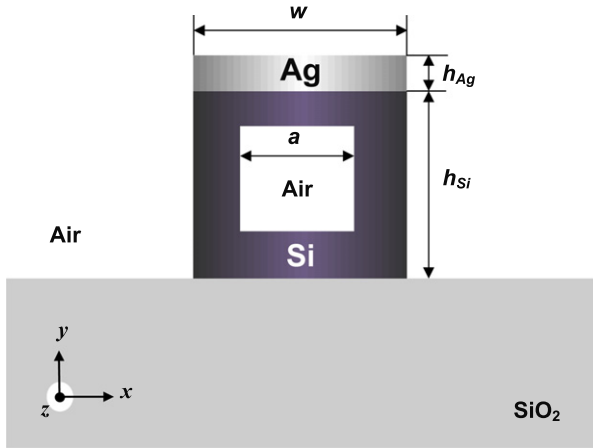


Figure 1. Schematic diagram of the studied metal-coated hollow nanowire plasmonic waveguide.

an air-filled slot [22, 26–28] between them, which is similar to the approach for extending the propagation length of long-range surface plasmons [37]. The formed hybrid plasmonic mode could feature both tight mode confinement and low propagation loss for a broad range of optical wavelengths. Here, in this work, we propose an alternative approach to balance the trade-off between the confinement and loss by using silicon nanowires with hollow cores instead of solid silicon nanowires. Pure silicon waveguides with similar hollow air core [38] or SiO₂-filled core [39] have been theoretically studied as slot structures for two-dimensional field enhancement and optical confinement. However, our simulation results demonstrate that, besides preserving the key advantages of silicon and metallic devices, the hollow nanowire based plasmonic waveguides offer new possibilities for both loss reduction and good mode confinement. We further show that, by introducing an additional buffer layer between the silicon wire and the metal coating, the structure could possess even lower propagation loss with a nanoscale mode area.

The proposed waveguides could be realized using modern fabrication methods. For example, to form the hollow nanowire, wafer bonding methods could be employed to connect a SOI wafer with a prepatterned square-shaped air nanotrench with a thin layer of silicon [38]. Lithography and etching procedures can then be applied to define the plasmonic waveguide of a finite-width after the buffer layer and the metallic coating were deposited on top of the silicon layer. For practical applications, in order to further ease the fabrication process, other semiconductor nanotubes (such as ZnO, ZnS) may also be used [17, 40], which are available using versatile chemical fabrication techniques.

2. Hollow nanowire based plasmonic waveguides: geometries and modal properties

2.1. Metal-coated hollow nanowire plasmonic waveguides

The schematic of the metal-coated hollow nanowire plasmonic waveguide is shown in figure 1, which consists

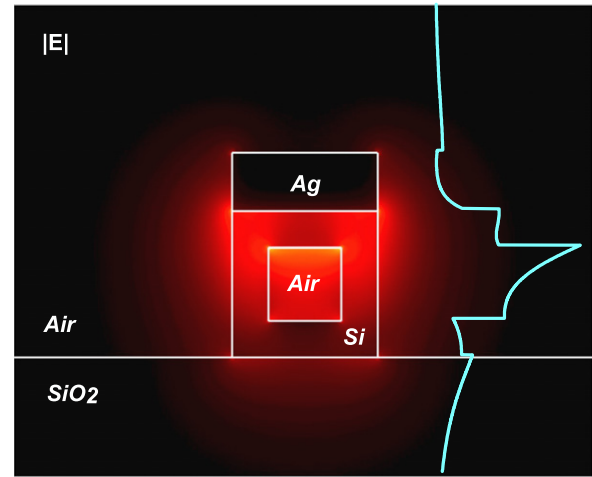


Figure 2. Electric field distribution of the fundamental plasmonic mode supported by the metal-coated hollow nanowire waveguide ($w = h_{Si} = 250$ nm, $r = 0.5$, $h_{Ag} = 100$ nm).

of a silver layer deposited directly over a hollow silicon nanowire on a silica substrate. The silver layer and the hollow nanowire have the same width of w . The heights of the silver layer and the hollow nanowire are h_{Ag} and h_{Si} , respectively. For simplicity, the hollow silicon nanowire and its air-filled hollow core (width and height: a) are assumed to have square cross-sections (i.e. $w = h_{Si}$). The width ratio r is given by a/w . In the following simulations, the wavelength is set at $\lambda = 1550$ nm. The permittivities of SiO₂, Si and Ag are $\epsilon_c = 2.25$, $\epsilon_d = 12.25$ and $\epsilon_m = -129 + 3.3i$ [41], respectively. The modal properties are investigated by means of the finite-element method (FEM) using COMSOLTM with the scattering boundary condition.

In the simulations, the height of the silver layer is fixed at 100 nm and w is chosen as 200, 250, 300 nm with varied hollow cores. Simulation results indicate that the studied metal-coated hollow nanowire waveguide can support a fundamental quasi-TM plasmonic mode under a wide range of geometric parameters. As an example, the electric field distribution of the fundamental plasmonic mode is drawn in figure 2, where w and r are chosen as 250 nm and 0.5, respectively. It is demonstrated that besides the enhancement at the Ag/Si interface, an even stronger local field enhancement could be observed in the hollow core region due to the slot effect [38, 42]. The cross-sectional curve of the electric field also indicates that, for the hollow core, the enhancement of the electric field is much more pronounced at the upper interface (near the metallic coating) than the lower interface (near the substrate). It is expected that the hollow core may contribute to the reduction of the propagation loss, while at the same time leading to weakened mode confinement, as indicated by the slight spreading of the electric field.

The calculated mode properties including the modal effective index (N_{eff}), propagation length (L_p) and normalized mode area (A_{eff}/A_0) of the fundamental hybrid plasmonic mode of the metal-coated hollow nanowire structures with different w are shown in figure 3 as r varies from 0 to

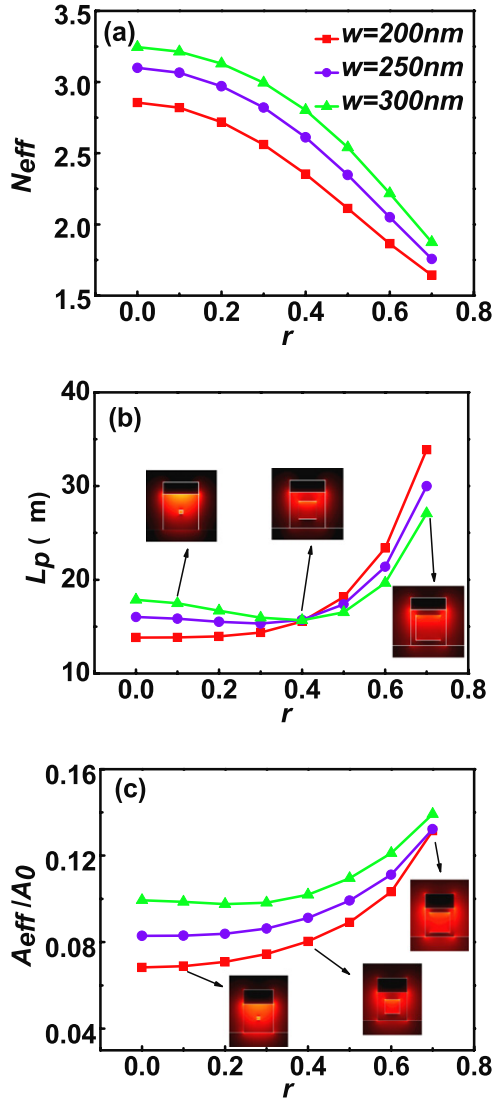


Figure 3. The dependence of modal properties on r : (a) the modal effective index (N_{eff}); (b) the propagation length (L_p). Insets show the electric field distributions of the hybrid plasmonic waveguides with $w = 300$ nm, $r = 0.1$; $w = 300$ nm, $r = 0.4$; $w = 300$ nm, $r = 0.7$; (c) the normalized mode area (A_{eff}/A_0). Insets show the electric field distributions of the hybrid plasmonic waveguides with $w = 200$ nm, $r = 0.1$; $w = 200$ nm, $r = 0.4$; $w = 200$ nm, $r = 0.7$.

0.7, where the extreme cases of $r = 0$ correspond to the metal-coated non-hollow waveguides. The modal effective index is obtained by calculating the ratio of the wavenumber of the waveguide mode to the free-space wavenumber. The propagation length is given by $L_p = \lambda/[4\pi \text{Im}(n_{\text{eff}})]$. A_0 is the diffraction-limited mode area defined as $\lambda^2/4$. The effective mode area (A_{eff}) is calculated using $A_{\text{eff}} = (\int \int W(r) dA)^2 / (\int \int W(r)^2 dA)$, where the definition of the electromagnetic energy density $W(r)$ is the same as that in [9, 43].

Figure 3(a) illustrates that N_{eff} drops monotonically when r gets bigger or w becomes smaller, while increased mode area indicating weakened confinement is observed with the increment of r or w . And such a trend gets more pronounced when the hollow core is relatively large, which is caused

by the rapid spreading of the field due to the dramatically reduced mode confinement, as also indicated in the electric field distributions drawn in the inset. Correspondingly, the propagation length also sees an increase with the expanding of the mode area when $w = 200$ nm. Calculation results also show that, for such a case, the propagation loss is smaller than the nanowire based plasmonic waveguides without hollow cores. However, different trends are observed at $w = 250$ nm or 300 nm, where L_p decreases first before it increases. It is also shown in figure 3(b) that a hollow nanowire with larger w suffers lower loss when $r < 0.4$, while a reverse trend occurs when $r > 0.4$, where smaller hollow nanowires have longer propagation lengths. The above phenomena observed in the curves of the propagation lengths are related to the different coupling strengths between the metal layer and silicon hollow nanowire at different sizes. When the effective index of the SPP mode matches that of the dielectric mode, the strongest coupling between them occurs, which leads to the occurrence of the largest propagation loss. That is why a minimum propagation length is observed when w is relatively large, while for small silicon nanostructure (e.g. $w = 200$ nm), its effective index is lower than that of the SPP's and would decrease further with the continuously enlarged hollow region. Correspondingly, the coupling strength between the two modes would also get weaker and consequently lead to a monotonic trend in the propagation length. As can be seen in figures 3(b) and (c), for the considered range of geometry parameters, sub-wavelength mode confinement could be achieved along with relatively long-range propagation distance. Further increasing of L_p could be realized by enlarging the size of the hollow core. However, when r is larger than 0.7, the studied hybrid mode is almost close to cut-off with N_{eff} approaching 1.5, which puts limitations on the further extension of the propagation distance. In order to achieve the goal of loss reduction, a second type of hollow nanowire based waveguide is proposed, which will be studied in the following section.

2.2. Metal-coated hollow nanowire hybrid plasmonic waveguides

In this section, we carry out a detailed analysis on the second type of waveguide, namely the metal-coated hollow nanowired hybrid plasmonic waveguide. It is schematically shown in figure 4, where an additional SiO_2 layer is introduced between the Ag layer and the Si hollow nanowire. The height of the SiO_2 buffer layer is denoted as h_b while other parameters are the same as those in figure 1. The modal properties are investigated by varying the thickness of the SiO_2 layer with different hollow nanowires. In the simulations, the height of the silver layer is fixed at 100 nm and w is chosen as 200, 250, 300 nm. As demonstrated by the numerical simulations, the hybrid plasmonic waveguide can also support a fundamental quasi-TM plasmonic mode under a wide range of geometric parameters, similar to the first type. Figure 5 shows the electric field distribution of the fundamental hybrid plasmonic mode of the structure when $w = 250$ nm with $r = 0.5$. It is seen that due to the strong

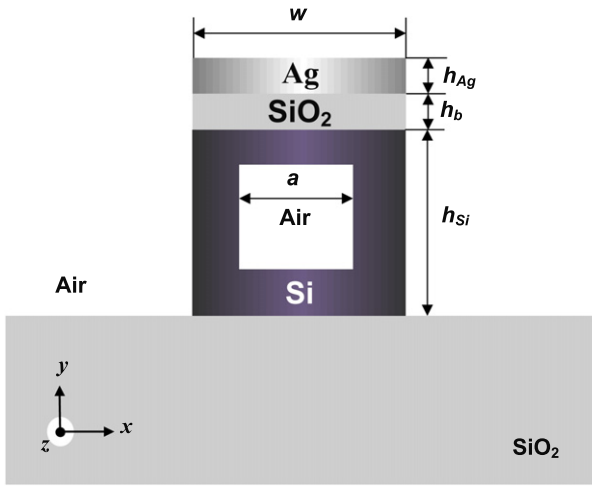


Figure 4. Schematic diagram of the studied metal-coated hollow nanowire hybrid plasmonic waveguide.

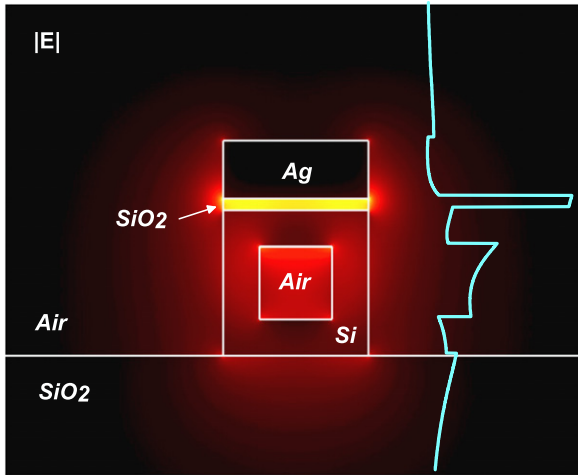


Figure 5. Electric field distribution of the fundamental hybrid plasmonic mode supported by the metal-coated hollow nanowire hybrid waveguide ($w = h_{Si} = 250$ nm, $r = 0.5$, $h_b = 20$ nm, $h_{Ag} = 100$ nm).

hybridization of the plasmonic mode and the dielectric mode of the hollow nanowire, the electric field is greatly enhanced in the low-index SiO₂ layer, which is much stronger than that in the hollow region of the Si nanowire. The introduced buffer layer, combined with the hollow core, is expected to be beneficial to the further reduction of the propagation loss, as the mode field distribution is further shifted away from the metal/Si interface and towards the low-index area.

Figure 6 shows the calculated modal properties at various buffer layer thicknesses with different hollow nanowires, where the case of $h_b = 0$ nm represents the first type of waveguide without the buffer layer. It is clearly seen that increasing h_b results in decreased N_{eff} as well as increased propagation length and larger effective mode area, which are also illustrated correspondingly in the electric field distributions depicted in the insets. Besides, the propagation length undergoes a more dramatic increase with the increment of h_b than the effective mode area, which is also illustrated

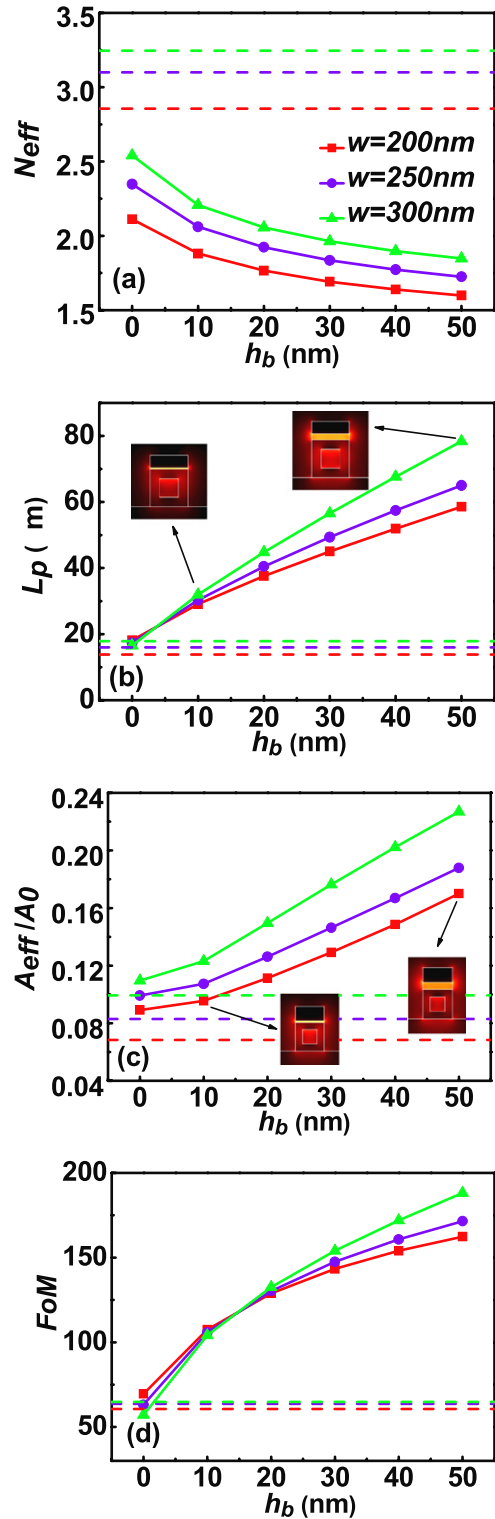


Figure 6. The dependence of modal properties on the thickness of the SiO₂ layer ($r = 0.5$): (a) the modal effective index (N_{eff}); (b) the propagation length (L_p). Insets show the electric field distributions of the hybrid plasmonic waveguides with $w = 300$ nm, $h_b = 10$ nm; $w = 300$ nm, $h_b = 50$ nm; (c) the normalized mode area (A_{eff}/A_0). Insets show the electric field distributions of the hybrid plasmonic waveguides with $w = 200$ nm, $h_b = 10$ nm; $w = 200$ nm, $h_b = 50$ nm; (d) the figure of merit (FoM). The modal characteristics of the waveguide with silver deposited directly on top of a non-hollow silicon nanowire are also plotted in the figures (see the dashed lines).

in the curve of the figure of merit (FoM) in figure 6(d). FoM is defined as the ratio of the propagation length (L_p) to the effective mode size (D_{eff}) [44], where D_{eff} is defined as the diameter of the effective mode area (A_{eff}), i.e. $D_{\text{eff}} = \sqrt{4A_{\text{eff}}/\pi}$. The calculated FoM clearly indicates improved optical performance achieved by introducing the buffer layer. Further reduction of the propagation loss could also be realized by tuning the size of the hollow core or increasing the thickness of the buffer layer. Here, it is also worth mentioning that for the metal-coated non-hollow waveguides ($r = 0$ in figure 3), more than one plasmonic mode can be supported by the structure when the silicon nanowire is relatively large (e.g. three modes exist when $w = 300$ nm). The multimode guiding might induce high modal dispersion, which could limit the operation bandwidth of such waveguides when used in transmission applications. By introducing the hollow air core (for the first type of proposed structures), the number of sustained modes can be greatly reduced (e.g. only two guided modes for $w = 300$ nm, $r = 0.5$). Even more modes can be suppressed by further employment of the buffer layer (i.e. for the second type). For instance, a metal-coated hybrid hollow waveguide with parameters of $w = 300$ nm, $r = 0.5$ and $h_b = 10$ nm has only one guided optical mode. Such a single-mode condition can also be readily achieved with other geometries by tuning the sizes of the hollow core and/or the buffer layer.

3. Conclusions

In this paper, the characteristics of two types of hollow nanowire based plasmonic waveguides are investigated at a wavelength of 1550 nm. Simulation results reveal that both of the two types of structures could support the low-loss propagation of plasmonic modes with small mode area. Compared to the metal-coated nanowire counterparts, the proposed metal-coated hollow nanowire structures with properly selected geometries exhibit lower propagation loss while keeping similar confinement capacity. On the other hand, the second type of waveguide, with additional buffer layer added between the metal layer and the hollow nanowire, shows improved optical performance over the first one, due to the formed efficient hybrid plasmonic modes. With these nice optical features as well as their easy-to-fabricate properties, both of the presented hollow nanowire based plasmonic waveguides could be useful candidates for integrated photonic circuits.

Acknowledgments

The work at Beihang University was supported by 973 Program (2009CB930701), NSFC (60921001/61077064), National Key Scientific Instruments and Equipment Development Special Fund Management (2011YQ0301240502) and the Innovation Foundation of BUAA for PhD Graduates.

References

[1] Barnes W L, Dereux A and Ebbesen T W 2003 Surface plasmon subwavelength optics *Nature* **424** 824–30

- [2] Gramotnev D K and Bozhevolnyi S I 2010 Plasmonics beyond the diffraction limit *Nature Photon.* **4** 83–91
- [3] Takahara J, Yamagishi S, Taki H, Morimoto A and Kobayashi T 1997 Guiding of a one-dimensional optical beam with nanometer diameter *Opt. Lett.* **22** 475–7
- [4] Berini P 2000 Plasmon-polariton waves guided by thin lossy metal films of finite width: bound modes of symmetric structures *Phys. Rev. B* **61** 10484–503
- [5] Boltasseva A, Nikolajsen T, Leosson K, Kjaer K, Larsen M S and Bozhevolnyi S I 2005 Integrated optical components utilizing long-range surface plasmon polaritons *J. Lightwave Technol.* **23** 413–22
- [6] Liu L, Han Z and He S 2005 Novel surface plasmon waveguide for high integration *Opt. Express* **13** 6645–50
- [7] Veronis G and Fan S H 2005 Guided subwavelength plasmonic mode supported by a slot in a thin metal film *Opt. Lett.* **30** 3359–61
- [8] Pile D F P, Ogawa T, Gramotnev D K, Matsuzaki Y, Vernon K C, Yamaguchi K, Okamoto T, Haraguchi M and Fukui M 2005 Two-dimensionally localized modes of a nanoscale gap plasmon waveguide *Appl. Phys. Lett.* **87** 261114
- [9] Dionne J A, Sweatlock L A, Atwater H A and Polman A 2006 Plasmon slot waveguides: towards chip-scale propagation with subwavelength-scale localization *Phys. Rev. B* **73** 035407
- [10] Bozhevolnyi S I, Volkov V S, Devaux E, Laluet J Y and Ebbesen T W 2006 Channel plasmon subwavelength waveguide components including interferometers and ring resonators *Nature* **440** 508–11
- [11] Pile D F P, Ogawa T, Gramotnev D K, Okamoto T, Haraguchi M, Fukui M and Matsuo S 2005 Theoretical and experimental investigation of strongly localized plasmons on triangular metal wedges for subwavelength waveguiding *Appl. Phys. Lett.* **87** 061106
- [12] Schmidt M and Russell P 2008 Long-range spiralling surface plasmon modes on metallic nanowires *Opt. Express* **16** 13617–23
- [13] Lee H, Schmidt M, Russell R, Joly N, Tyagi H, Uebel P and Russell P S J 2011 Pressure-assisted melt-filling and optical characterization of Au nano-wires in microstructured fibers *Opt. Express* **19** 12180–9
- [14] Steinberger B, Hohenau A, Ditzbacher H, Stepanov A L, Drezet A, Aussenegg F R, Leitner A and Krenn J R 2006 Dielectric stripes on gold as surface plasmon waveguides *Appl. Phys. Lett.* **88** 094104
- [15] Holmgaard T and Bozhevolnyi S I 2007 Theoretical analysis of dielectric-loaded surface plasmon-polariton waveguides *Phys. Rev. B* **75** 245405
- [16] Oulton R F, Sorger V J, Genov D A, Pile D F P and Zhang X 2008 A hybrid plasmonic waveguide for subwavelength confinement and long-range propagation *Nature Photon.* **2** 496–500
- [17] Sorger V J, Ye Z, Oulton R F, Wang Y, Bartal G, Yin X and Zhang X 2011 Experimental demonstration of low-loss optical waveguiding at deep sub-wavelength scales *Nature Commun.* **2** 331
- [18] Dai D X and He S L 2009 A silicon-based hybrid plasmonic waveguide with a metal cap for a nano-scale light confinement *Opt. Express* **17** 16646–53
- [19] Bian Y S, Zheng Z, Zhao X, Zhu J S and Zhou T 2009 Symmetric hybrid surface plasmon polariton waveguides for 3D photonic integration *Opt. Express* **17** 21320–5
- [20] Avrutsky I, Soref R and Buchwald W 2010 Sub-wavelength plasmonic modes in a conductor-gap-dielectric system with a nanoscale gap *Opt. Express* **18** 348–63
- [21] Alam M Z, Meier J, Aitchison J S and Mojahedi M 2010 Propagation characteristics of hybrid modes supported by metal-low-high index waveguides and bends *Opt. Express* **18** 12971–9

- [22] Bian Y S, Zheng Z, Liu Y, Zhu J S and Zhou T 2010 Dielectric-loaded surface plasmon polariton waveguide with a holey ridge for propagation-loss reduction and subwavelength mode confinement *Opt. Express* **18** 23756–62
- [23] Chen D R 2010 Cylindrical hybrid plasmonic waveguide for subwavelength confinement of light *Appl. Opt.* **49** 6868–71
- [24] Bian Y S, Zheng Z, Liu Y, Liu J S, Zhu J S and Zhou T 2011 Hybrid wedge plasmon polariton waveguide with good fabrication-error-tolerance for ultra-deep-subwavelength mode confinement *Opt. Express* **19** 22417–22
- [25] Ta V D, Chen R and Sun H D 2011 Wide-range coupling between surface plasmon polariton and cylindrical dielectric waveguide mode *Opt. Express* **19** 13598–603
- [26] Bian Y S, Zheng Z, Liu Y, Zhu J S and Zhou T 2011 Coplanar plasmonic nanolasers based on edge-coupled hybrid plasmonic waveguides *IEEE Photon. Technol. Lett.* **23** 884–6
- [27] Su Y L, Zheng Z, Bian Y S, Liu Y, Liu J S, Zhu J S and Zhou T 2011 Low-loss silicon-based hybrid plasmonic waveguide with an air nanotrench for sub-wavelength mode confinement *Micro Nano Lett.* **6** 643–5
- [28] Xiao J, Liu J S, Zheng Z, Bian Y S and Wang G J 2011 Design and analysis of a nanostructure grating based on a hybrid plasmonic slot waveguide *J. Opt.* **13** 105001
- [29] Krasavin A V and Zayats A V 2010 Silicon-based plasmonic waveguides *Opt. Express* **18** 11791–9
- [30] Lipson M 2005 Guiding, modulating, and emitting light on silicon—challenges and opportunities *J. Lightwave Technol.* **23** 4222–38
- [31] Wu M, Han Z H and Van V 2010 Conductor-gap-silicon plasmonic waveguides and passive components at subwavelength scale *Opt. Express* **18** 11728–36
- [32] Chu H S, Li E P, Bai P and Hegde R 2010 Optical performance of single-mode hybrid dielectric-loaded plasmonic waveguide-based components *Appl. Phys. Lett.* **96** 221103
- [33] Zhu S Y, Liow T Y, Lo G Q and Kwong D L 2011 Silicon-based horizontal nanoplasmonic slot waveguides for on-chip integration *Opt. Express* **19** 8888–902
- [34] Song Y, Wang J, Yan M and Qiu M 2011 Subwavelength hybrid plasmonic nanodisk with high Q factor and Purcell factor *J. Opt.* **13** 075001
- [35] Kim J T 2011 CMOS-compatible hybrid plasmonic slot waveguide for on-chip photonic circuits *IEEE Photon. Technol. Lett.* **23** 1481–3
- [36] Kwon M S 2011 Metal–insulator–silicon–insulator–metal waveguides compatible with standard CMOS technology *Opt. Express* **19** 8379–93
- [37] Adato J G R and Guo J 2006 Extended long range plasmon waves in finite thickness metal film and layered dielectric materials *Opt. Express* **14** 12409–27
- [38] Lim S T, Png C E and Danner A J 2010 Embedded air core optical nano-waveguides *J. Opt. Soc. Am. B* **27** 1937–41
- [39] Khanna A, Saynatjoki A, Tervonen A, Norwood R A and Honkanen S 2010 Polarization properties of two-dimensional slot waveguides *Appl. Opt.* **49** 5321–32
- [40] Zhang X Y, Hu A, Zhang T, Xue X J, Wen J Z and Duley W W 2010 Subwavelength plasmonic waveguides based on ZnO nanowires and nanotubes: a theoretical study of thermo-optical properties *Appl. Phys. Lett.* **96** 043109
- [41] Johnson P B and Christy R W 1972 Optical constants of the noble metals *Phys. Rev. B* **6** 4370–9
- [42] Almeida V R, Xu Q F, Barrios C A and Lipson M 2004 Guiding and confining light in void nanostructure *Opt. Lett.* **29** 1209–11
- [43] Oulton R F, Bartal G, Pile D F P and Zhang X 2008 Confinement and propagation characteristics of subwavelength plasmonic modes *New J. Phys.* **10** 105018
- [44] Buckley R and Berini P 2007 Figures of merit for 2D surface plasmon waveguides and application to metal stripes *Opt. Express* **15** 12174–82